

This work was written as part of one of the author's official duties as an Employee of the United States Government and is therefore a work of the United States Government. In accordance with 17 U.S.C. 105, no copyright protection is available for such works under U.S. Law.

Public Domain Mark 1.0

<https://creativecommons.org/publicdomain/mark/1.0/>

Access to this work was provided by the University of Maryland, Baltimore County (UMBC) ScholarWorks@UMBC digital repository on the Maryland Shared Open Access (MD-SOAR) platform.

Please provide feedback

Please support the ScholarWorks@UMBC repository by emailing scholarworks-group@umbc.edu and telling us what having access to this work means to you and why it's important to you. Thank you.

Atmospheric Chlorine and Stratospheric Ozone Nonlinearities and Trend Detection

J. R. HERMAN AND C. J. MCQUILLAN

Atmospheric Chemistry and Dynamics Branch, NASA Goddard Space Flight Center, Greenbelt, Maryland

The percent decrease of total stratospheric ozone column content due to the injection of fluorocarbons (F-11 and F-12) has been found to be a nearly linear function of the atmospheric mixing ratio of ClX between 1.2 and 10 parts per billion by volume (ppbv). In contrast, Cicerone et al. (1983) found a broad region of slightly positive change in ozone column content between 10 and 80 km for small ClX perturbations in addition to a nonlinear negative decrease for larger perturbations. The presence of a nonlinear response in column ozone to moderate ClX changes appears to depend strongly on the method of diurnal averaging employed in the calculation. The immediate decrease in ozone column content for our small ClX perturbation results leads to the prediction of an earlier date for possible experimental detection of total ozone trends related to chlorine. For larger ClX perturbations the response in column ozone is nonlinear when the amount of ClX in the stratosphere becomes comparable to or larger than the amount of NO_x . On the basis of our time-dependent calculations using a specified rate of fluorocarbon injection obtained from Logan et al. (1978), and similar previously obtained results from other models, the first evidence of an ozone decrease induced by ClX may be observable in the vicinity of 40 km by 1987-1990 with present-day satellite instrumentation (Nimbus 7). The actual detection of an ozone decrease by 1990 might be obscured by seasonal and longer-term atmospheric variations. Because of increasing fluxes of several minor constituents (e.g., CH_4), possible long-term temperature changes in the stratosphere, and possible secular solar flux changes, observation of an ozone decrease is not necessarily an indicator of damage to ozone caused by atmospheric chlorine. Comparing the percent difference curves near 40 km for the diurnal variation of ozone corresponding to different amounts of ClX may provide a means of distinguishing ClX effects from other atmospheric changes. The change should be detectable when ClX finally reaches 5 ppbv in the upper stratosphere (about 2020). By the year 2020 the total ozone decrease due to ClX should be about 3% (2.5% with increasing methane) and may already pose environmental problems.

INTRODUCTION

At the present time there is no experimental means to detect the current reduction of stratospheric ozone by chlorine from fluorocarbons relative to its unperturbed amount in view of the small changes involved and several possible masking effects. As a substitute for experimental detection, there have been many stratospheric modeling efforts since the original paper by Molina and Rowland [1974] to predict the amount of ozone change corresponding to specified rates of chlorine injection from ground sources. The history of these attempts has been reviewed in the recent papers by Cicerone et al. [1983] (hereinafter designated CWL) and by Wuebbles [1983]. It is sufficient to say here that the earlier calculations showed differing amounts of decrease in the ozone column content with increasing mixing ratio of atmospheric chlorine, depending on the chemistry reaction rates available at the time. After investigating several of these alternate sets of reaction rates to study the sensitivity of the calculation to some uncertainties in the photochemistry, CWL selected a likely current set of rates and found that the column ozone response was nonlinear and increasing slightly for small ClX perturbations (from 1.2 to about 4.2 parts per billion by volume (ppbv) of ClX), and then decreasing at a rate faster than linear for larger perturbations. Their predicted initial nearly flat region of increase in atmospheric ozone content lasting beyond the year 2005 implies that the successful detection of net ozone destruction by chlorine would be delayed many years from the present time.

In this paper we reinvestigate the photochemical problem

discussed by CWL on the basis of an independent one-dimensional model [Herman, 1979a, b]. A comparison is made between the response of the percentage change in ozone column content in the present model and the nonlinear response obtained by CWL. Because we obtain neither their nearly flat region of positive change in ozone column content for small chlorine perturbations nor their nonlinear change for larger perturbations, we discuss possible model differences that might account for our prediction of a linear decrease from the initial conditions.

In the present model, as in all others, the largest percentage decreases are predicted in the vicinity of 40 km altitude. The model results differ mainly in their predictions of the exact percentage decrease for a given amount of stratospheric ClX, and therefore the estimated date when experimental detection of the predicted ozone decrease can be achieved. On the basis of the amount of OH and HO_2 calculated in the upper stratosphere, we show that our predictions of ozone decrease above 40 km and those of CWL are likely to be the same.

The altitude range between 35 and 40 km is also the most sensitive region for detection of ozone changes using UV backscatter data from the Nimbus 7 satellite or other similar proposed instruments on future satellites. On the basis of model predictions alone, experimental detection of the high-altitude ozone reduction in response to increasing amounts of stratospheric ClX should be possible within a few years. We discuss the difficulties in detecting these changes within a given latitude band based on some of the likely long- and short-period variations also present in the ozone data. Since these masking effects make the association of an observed ozone change with atmospheric ClX uncertain, we discuss a possible means to obtain a unique measure of the ClX effect in the diurnal variation of ozone near 40 km.

This paper is not subject to U.S. copyright. Published in 1985 by the American Geophysical Union.

Paper number 5D0018.

MODEL DESCRIPTION

The stratospheric photochemistry model used for this study is an extension of the one-dimensional time-dependent model of Herman [1979a, b]. The model yields time-dependent solutions of the continuity equations for each chemical species in the atmosphere aside from N_2 and O_2 over an altitude range from 0 to 120 km. The N_2 and O_2 densities are calculated from the temperature and their boundary values by assuming that the usual hydrostatic pressure balance is applicable. Gas phase water density in the troposphere is adjusted to match the data of Kley *et al.* [1979] from the ground to 12.5 km by balancing the water vapor rain-out rate for the given eddy diffusion coefficient profile. Above 12.5 km its density is controlled by diffusion and photochemistry. For this study we solved 65 species equations using the chemistry rates specified by CWL for their case M. Additional chemical rates for those reactions not explicitly given by CWL were taken from NASA/Jet Propulsion Laboratory (JPL) [1982]. No assumptions were made about chemical families or the relative importance of the many minor reactions included in the present calculations. Photolysis rates were calculated from cross sections given by NASA/JPL [1982] except for O_2 in the Herzberg continuum and the Schumann-Runge band regions. The O_2 Herzberg continuum cross sections are based on the recent measurements of Herman and Mentall [1982], and the O_2 Schumann-Runge cross sections are obtained from the approximation given by Allen and Frederick [1982] without correction for the lower Herzberg continuum cross sections.

Boundary conditions for each species were specified at the ground and 120 km altitude so as to yield conditions that approximate those of CWL given at 10 and 80 km. The lower boundary (0 km) values for some of the chemical species are H_2 (0.5 parts per million by volume (ppmv)), CH_4 (1.5 ppmv), CO (73 ppbv), N_2O (300 ppbv), CCl_4 (0.13 ppbv), and CH_3Cl (0.68 ppbv). Many of the others are found from the requirement of pure chemical balance (e.g., NO_3 , N_2O_5 , CH_3O , H , HO_2 , NO , Cl , ClO , O , $O(^1D)$) at the ground. Two assumed versions of the eddy diffusion coefficients were used as shown in Table 1. All but two of the cases described in the figures are based on the coefficient K_0 , and the remaining two were computed using an approximation to K_2 of CWL. Solar fluxes were taken from the World Meteorological Organization [1981] at the wavelength intervals specified by Ackerman [1971] except in the Schumann-Runge band region where a wavelength interval is assigned to each of 19 bands. Within the atmosphere the attenuated and scattered fluxes were computed from a two-stream version of the matrix operator method described by Plass *et al.* [1973] with spherical geometry corrections applied to the effective optical depth. These calculations have been demonstrated to compare well with experimental data [Herman and Mentall, 1982].

The two basic types of solutions obtained are (1) fully time-dependent solutions showing the diurnal variations of each species and (2) time-dependent diurnally averaged solutions for longer-time scale phenomena or steady state solutions. The diurnal averaging of the solar fluxes is obtained from the formulation of Rundel [1977] except for cases such as the calculation within the Schumann-Runge bands where the 24-hour averages are explicitly calculated for each band and altitude using the formulation of Allen and Frederick [1982] for the pressure and temperature-dependent effective cross sections. The diurnal averaging of photolysis and kinetic reaction rates is accomplished by calculating the numerical 24-hour

TABLE 1. Temperature and Eddy Coefficient

Altitude, km	Temperature, °K	K_2 , cm ² /s	K_0 , cm ² /s
0.00	288.10	2.67×10^5	2.67×10^5
1.25	280.00	2.40×10^5	2.40×10^5
2.50	271.60	2.08×10^5	2.08×10^5
5.00	255.70	1.62×10^5	1.62×10^5
7.50	239.50	1.26×10^5	1.26×10^5
10.00	223.20	9.82×10^4	9.82×10^4
12.50	219.20	7.65×10^4	7.65×10^4
15.00	213.50	1.00×10^4	1.00×10^4
17.50	211.10	7.70×10^3	7.70×10^3
20.00	211.70	5.80×10^3	5.80×10^3
22.50	212.50	8.20×10^3	8.80×10^3
25.00	216.00	1.05×10^4	1.50×10^4
27.50	220.00	1.60×10^4	1.65×10^4
30.00	226.50	2.60×10^4	1.90×10^4
35.00	236.50	5.00×10^4	2.50×10^4
40.00	250.40	1.30×10^5	3.40×10^4
45.00	264.20	2.90×10^5	4.50×10^4
50.00	270.60	6.00×10^5	6.00×10^4
55.00	260.80	8.60×10^5	8.00×10^4
60.00	247.00	1.13×10^6	1.05×10^5
65.00	233.30	1.35×10^6	1.40×10^5
70.00	219.60	1.55×10^6	1.90×10^5
75.00	208.40	1.68×10^6	2.50×10^5
80.00	198.60	1.73×10^6	3.30×10^5
85.00	188.90	1.70×10^6	4.40×10^5
90.00	186.90	1.62×10^6	5.80×10^5
95.00	188.40	1.45×10^6	7.40×10^5
100.00	195.10	1.20×10^6	8.60×10^5
105.00	208.80	9.20×10^5	8.00×10^5
110.00	240.00	6.80×10^5	6.80×10^5
120.00	360.00	4.00×10^5	4.00×10^5

The eddy coefficient K_0 is an adjusted altitude-dependent function selected to produce as good a fit as possible between diffusion-dominated species (e.g., N_2O , F-11, F-12, CCl_4 , etc.) and available data [World Meteorological Organization, 1981]. K_2 is approximated from Cicerone *et al.* [1983] for the range 20 to 80 km and joined smoothly to K_0 for other altitudes between 0 and 120 km.

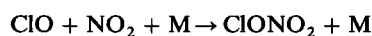
average of each reaction product, $J[X]$, $K[X][Y]$, or $K[X][Y][Z]$, at each altitude from the fully time-dependent model. A set of these averages is computed for each new case by iterating between the time-dependent and steady state solutions. The resulting tables provide the basis for a fast and accurate method of obtaining diurnally averaged solutions without approximations.

The solutions for most species densities are obtained using the methods described by Herman [1979a]. A multidimensional Newton-Raphson iteration matrix is constructed with the Jacobian of the system determined analytically at each time step. The simultaneous solution of the chemical continuity equations by this method avoids "stiffness" problems and yields solutions that can be made as accurate as desired within the limits of the computer word size. A few of the species whose solutions are dominated by the diffusion terms in their continuity equations (e.g., H_2 , CO_2 , CH_4) are solved using the Crank-Nicholson approach [Carnahan *et al.*, 1969]. This has been found to speed up the integration procedure to obtain a given accuracy. Combining the two different integration techniques is particularly useful at altitudes above 75 km, where binary diffusion effects start, to the present upper boundary at 120 km. Typically, when the final solutions are obtained at a given step and simultaneously resubstituted into the entire system of equations, the largest residual indicates eight figures of accuracy. When steady state solutions are desired, the time-dependent equations are integrated using a large time step

(e.g., 100 days) until convergence is achieved in the fifth significant figure when changes to the 0.1% level are considered significant for the problem under discussion.

RESULTS

The chemistry options specified by CWL as their cases K, L, M, and N use more current reaction rates than most of the other cases discussed by CWL. In addition, for CWL, cases L and M produced a broad region of increase in total ozone column content $C(O_3)$, with increases in atmospheric chlorine content from 1.16 ppbv to about 4 ppbv. Because the use of current reaction rates produces the prediction of a long delay in the possible detection of ozone depletion by CIX, we have selected one of the two cases, case M, for our study. In addition to several minor changes in our standard set of reaction rates, two key rates were modified in the current model to match the rates in case M (all reaction rates are in cgs units, cm^3/s , cm^6/s , or s^{-1}):



where K is the NASA/JPL [1982] fast rate, and



A series of steady state solutions for ozone with differing amounts of atmospheric chlorine were obtained using case M chemistry and the eddy coefficient K_0 given in Table 1. As in the work by CWL, only the mixing ratios of CFCl_3 and

TABLE 2. Chlorocarbon Boundary Conditions Mixing Ratio

Year	CF_2Cl_2	CFCl_3	CH_3CCl_3
1950	0.0000	0.0000	0.0039
1955	0.0020	0.0000	0.0039
1960	0.0259	0.0097	0.0039
1965	0.0804	0.0473	0.0095
1970	0.1364	0.0754	0.0155
1975	0.1947	0.1120	0.0320
1980	0.2625	0.1567	0.0496
1985	0.3584	0.2185	0.0685
1990	0.4442	0.2725	0.0873
1995	0.5293	0.3250	0.1052
2000	0.6129	0.3854	0.1230
2005	0.6816	0.4257	0.1396
2010	0.7503	0.4654	0.1555
2015	0.8084	0.5060	0.1732
2020	0.8644	0.5463	0.1940
2025	0.9253	0.5848	0.2147
2030	0.9859	0.6205	0.2364
2035	1.0462	0.6452	0.2603
2040	1.1018	0.6699	0.2841
2045	1.1472	0.6931	0.3086
2050	1.1926	0.7156	0.3342
2055	1.2436	0.7387	0.3598
2060	1.2962	0.7631	0.3787
2065	1.3444	0.7846	0.3929
2070	1.3924	0.8043	0.4069
2075	1.4391	0.8198	0.4185
2080	1.4846	0.8315	0.4305
2085	1.5283	0.8465	0.4474
2090	1.5706	0.8627	0.4644
2095	1.6098	0.8789	0.4860
2100	1.6500	0.8900	0.5080

Values are in parts per billion by volume. The mixing ratios at 0 km altitude for F-11, F-12, and CH_3CCl_3 are given as a function of time for model B2 of Logan *et al.* [1978], where the data are taken directly from their Figure 39. Use of these boundary conditions and the present model calculation leads to a value of CIX that is slightly smaller than shown by CWL. The small CIX differences arise mainly from the use of different eddy coefficients.

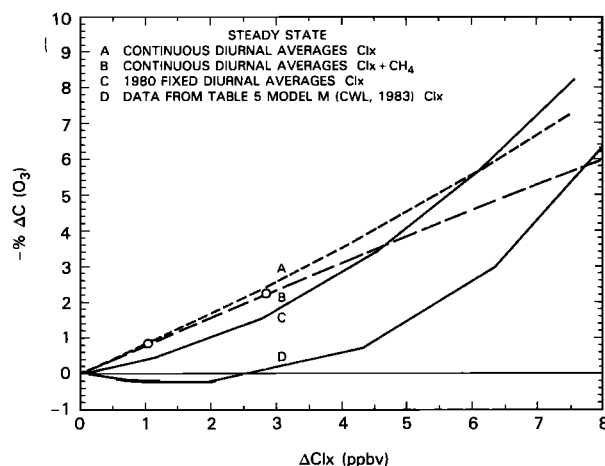


Fig. 1. The change in column ozone from 10 to 120 km and 40 to 120 km as a function of the amount of CIX at 55 km obtained from a series of steady state solutions for continuously recomputed diurnal averages (curves A and B) and a fixed set of diurnal averages (curve C). Curves A and C are for a CIX perturbation, whereas curve B is for a combined CIX and CH_4 perturbation as discussed in reference to Figure 6. The reference cases have 1.22 ppbv of CIX at 55 km. The curves A, B, and C are computed using the eddy coefficient $K = K_0$ and the reaction rate $a_7 = 3.0 \times 10^{-11} e^{200/T} \text{ cm}^3/\text{s}$ for $\text{HO}_2 + \text{O} \rightarrow \text{O}_2 + \text{OH}$. The two points labeled with circles have $K = K_2$ and $a_7 = 4.0 \times 10^{-11} \text{ cm}^3/\text{s}$ as suggested by CWL. Curve D is copied from Table 5, model M, of CWL.

CF_2Cl_2 were varied, with CH_3Cl and CCl_4 being held constant at 0.68 and 0.13 ppbv respectively. The mixing ratios of F-11 and F-12 (CFCl_3 and CF_2Cl_2) were taken from model B2 of Logan *et al.* [1978] with the chlorine content of CH_3CCl_3 being added to CFCl_3 (see Table 2).

Prior to the introduction of fluorocarbons into the atmosphere, the CIX mixing ratio was about 1.22 ppbv based on the boundary conditions suggested by Logan *et al.* [1978]. The calculated ozone density profiles corresponding to 1.22 ppbv of CIX are taken to be the reference values for computing the amount of ozone depletion due to differing amounts of CIX. The resulting percent changes in column content of ozone from 10 to 120 km as functions of the CIX mixing ratio at 55 km ($\mu[\text{HCl}] + \mu[\text{Cl}] + \dots$) are shown in Figure 1 (plots labeled A and C). Cases A and C are identical except for the method of diurnal averaging of the chemical reaction and photolysis rates. For case A the diurnal averages were computed for each CIX mixing ratio point on the plot, whereas for case C a single set of diurnal averages was used, corresponding to CIX at 55 km having a mixing ratio of 2.37 ppbv (approximately 1980 conditions). As is shown later, most of the effect of continually updating the diurnal averages appears in the region below about 27 km. The resulting ozone changes in this region give rise to the nonlinearity shown in case C. We have also repeated the calculations for case A using the more recent chemistry rate evaluation [NASA/JPL, 1983]. The calculated ozone depletion was slightly larger (2.40% versus 2.38% for CIX = 3.99 ppbv).

On the basis of these solutions it is clear that we do not obtain the nearly zero slope region of positive ozone percent change found by CWL as the CIX content of the atmosphere is increased. Since the explanation for the region of positive change offered by CWL was partly based on one-dimensional transport effects, we modified our eddy coefficient to match K_2 of CWL between 20 and 80 km (see Table 1). We also modified the rate for $\text{HO}_2 + \text{O}$ to match CWL ($a_7 = 4 \times 10^{-11} \text{ cm}^3/\text{s}$). The results shown in Figure 1 by the small

circles indicate that the percentage change in total ozone column content is only weakly dependent on the choice of eddy coefficient and the rate a_7 . This should be expected since the two eddy coefficients are the same from the ground to 22.5 km so that the fluxes of most constituents into and out of the troposphere and lower stratosphere are only slightly altered. Above 30 km, ozone is increasingly controlled by the local chemistry. The net result is that the ozone density is the same to within a few percent up to about 50 km, leaving the total ozone column content nearly unchanged as shown in Figure 2.

Figure 2 compares the altitude dependence of using the larger eddy coefficient K_2 and the smaller modified rate for $\text{HO}_2 + \text{O}$ with using K_0 and the larger temperature-dependent rate as recommended by NASA/JPL [1982] for $\mu(\text{ClX}) = 2.37$ ppbv. As mentioned above, because of the near equality of K_0 and K_2 below 30 km, the differing eddy coefficients only contribute a small fraction of the calculated ozone change. In the upper stratosphere, and particularly above 50 km, the larger eddy coefficient K_2 results in more CH_4 and H_2O , and therefore in more HO_x . The increased HO_x reduces the ozone in the upper stratosphere and mesosphere with the maximum percentage decrease centered on about 90 km. The use of the smaller $\text{HO}_2 + \text{O}$ rate reduces the destruction of odd oxygen while producing no net change in HO_x . This leads to increased O_3 throughout most of the upper stratosphere until the increased HO_x from the use of the larger eddy coefficient reduces the ozone density in the mesosphere.

Figure 3 compares the changes in ozone density and column content between the two cases in Figure 2 ($\mu(\text{ClX}) = 2.37$ ppbv) and their respective reference cases ($\mu(\text{ClX}) = 1.22$ ppbv) as a function of altitude. The increased amount of ClX causes the ozone density to increase slightly below 30 km and then decrease between 30 and 70 km. The decrease above 30 km is large enough to dominate the increase below 30 km when calculating the ozone column content above 10 km for both cases. As mentioned earlier, our calculated decrease in $C(\text{O}_3)$ for small values of ClX is in disagreement with the results of CWL, both when we use their

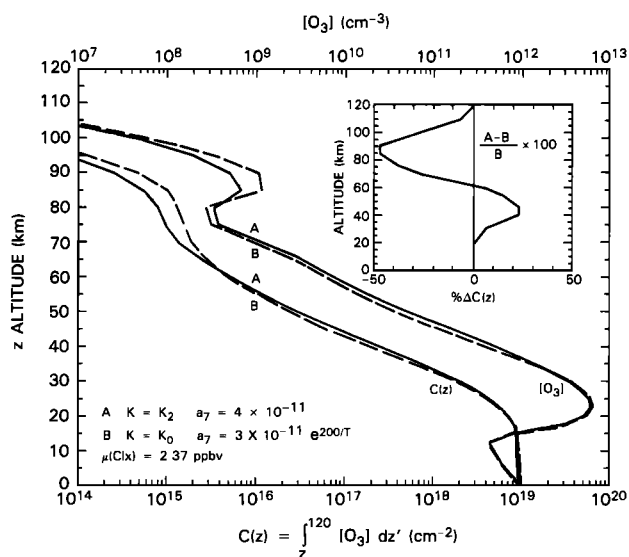


Fig. 2. The steady state ozone density and column content altitude profiles for two different values of the eddy coefficient and the rate for $\text{HO}_2 + \text{O} \rightarrow \text{O}_2 + \text{OH}$, $3.0 \times 10^{-11} e^{200/T} \text{ cm}^3/\text{s}$ with $K = K_0$ and $4.0 \times 10^{-11} \text{ cm}^3/\text{s}$ with $K = K_2$. The inset shows the percentage change in column ozone between the two cases with the case using K_0 as the reference ($100(C_2 - C_0)/C_0$).

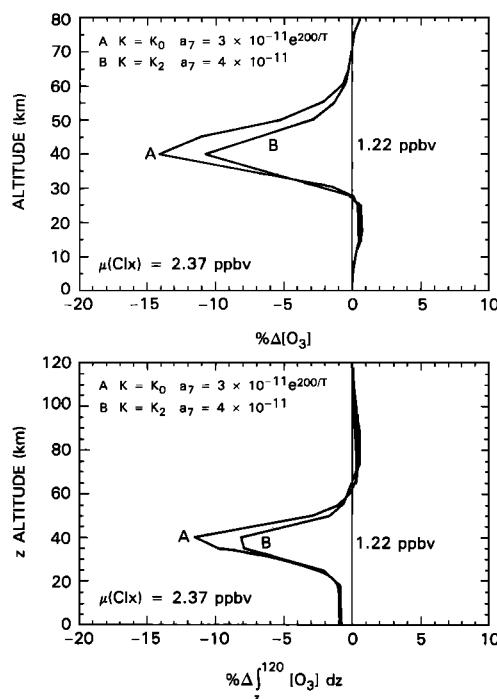


Fig. 3. The percent change in steady state ozone density and column ozone above the indicated altitude for the two cases shown in Figure 2 with $\text{ClX} = 2.37$ ppbv at 55 km relative to $\text{ClX} = 1.22$ ppbv. Both cases show a net decrease in column ozone throughout the troposphere and stratosphere. The small increase in $C(\text{O}_3)$ in the mesosphere arises from a small decrease in HO_x .

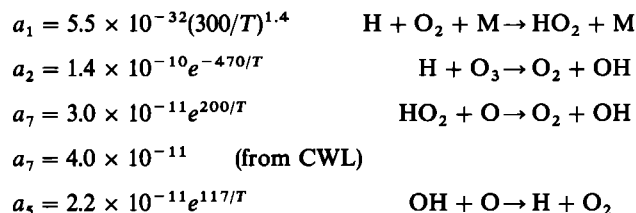
choices of eddy coefficient and $\text{HO}_2 + \text{O}$ reaction rate and when we use K_2 and the faster reaction rate.

In order to examine possible differences between the present model calculations with those of CWL that might give rise to the above disagreement, two plots of the noontime mixing ratios of OH , HO_2 , ClO , HOCl , HCl , ClONO_2 , and HO_2NO_2 are given in Figures 4a and 4b when $\mu(\text{ClX})$ is 2.37 ppbv (compare with Figure 4b of CWL). Figure 4a is based on the chemistry rates and eddy coefficients K_2 for case M of CWL. Figure 4b uses K_0 and the same chemistry rates except for the NASA/JPL [1982] rate for $\text{HO}_2 + \text{O} \rightarrow \text{O}_2 + \text{OH}$. The different chemical rates used in the two cases lead to the ratio $[\text{OH}]/[\text{HO}_2]$ being approximately 2.19 at 55 km in Figure 4b and 1.38 in Figure 4a. The two different ratios arise primarily from the use of a temperature-independent reaction rate for $\text{HO}_2 + \text{O}$ adopted by CWL instead of the rate given by NASA/JPL [1982], and from the dependence of the O_3 mixing ratio on the assumed eddy coefficient (K_2 in Figure 4a and K_0 in Figure 4b).

The analytical expression for the chemical equilibrium value of the $[\text{OH}]/[\text{HO}_2]$ ratio is [Nicolet, 1975, equation 58]

$$\frac{[\text{OH}]}{[\text{HO}_2]} = \frac{a_7 a_1 [\text{M}][\text{O}_2] + a_2 [\text{O}_3]}{a_5 a_1 [\text{M}][\text{O}_2]} \quad (1)$$

where the rates are from NASA/JPL [1982],



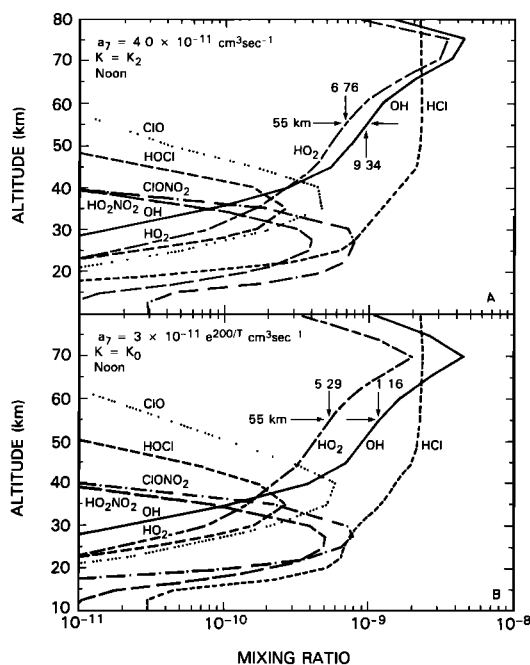


Fig. 4. The noontime mixing ratios of ClO, HOCl, OH, HO_2 , and HCl showing the effect of assuming different values for the $\text{HO}_2 + \text{O} \rightarrow \text{O}_2 + \text{OH}$ reaction rate on the OH/ HO_2 ratio at 55 km. Also shown in Figure 4a are the mixing ratios of ClONO_2 and HO_2NO_2 for comparison with the ratios of CWL. The results shown here compare well with those shown in Figure 5b of CWL showing the near equivalence of the models in the time-dependent mode without diurnal averaging.

When the calculated values of the ozone density at 55 km for the two cases are used ($1.38 \times 10^{10} \text{ cm}^{-3}$ for Figure 4b and $1.66 \times 10^{10} \text{ cm}^{-3}$ for Figure 4a), equation (1) yields 2.16 for Figure 4b and 1.38 for Figure 4a. From the data at 55 km in Figure 4b of CWL the $[\text{OH}]/[\text{HO}_2]$ ratio is $10.1/7.31 = 1.38$, exactly in agreement with the present model results and chemical equilibrium. The $[\text{OH}]/[\text{HO}_2]$ agreement indicates that both model calculations yield the same ozone mixing ratio in the upper stratosphere and mesosphere. A rough comparison of the mixing ratios of HO_2NO_2 and ClONO_2 with those given by CWL (see their Figure 6b) shows that the two models are in apparent agreement in the lower stratosphere. CWL's Figure 6b is for conditions different from those used for the present Figure 4a (sunset and 2.44 ppbv of CIX, compared to noontime and 2.37 ppbv of CIX). The mixing ratios of HO_2NO_2 and ClONO_2 are sensitive to the boundary conditions and densities of other species involved in the NO_x chemistry, indicating that no major disagreement between the two time-dependent models seems to be present. In summary, it would appear that the differences between the two models do not arise from the treatment of the chemical terms without diurnal averaging in the equations describing the atmosphere.

Among the possible sources for disagreement with the CIX perturbation results of CWL is that there may be a sensitivity to differences in the methods of calculating the solutions to the equations even though the mathematical basis is similar. The effects of using different solution methods are mainly in the treatment of the transport terms. Vertical transport effects are important below about 27 km, which is the same region that gives rise to the calculated nonlinear response of ozone to the CIX perturbation shown in Figure 1, case C. Both our central finite difference numerical representation of the transport terms and that of CWL have small but different truncation errors. Since both numerical representations of the trans-

port terms are consistent with the original differential equations, it is unlikely that the omitted higher-order terms are contributing to the solutions in a manner that accounts for the disagreement between the two models.

In addition to the transport terms, some other known differences between the two models are as follows: (1) The boundary conditions are specified as fixed mixing ratios at the ground, whereas CWL use specified fluxes at 10 km. (2) The temperature profile is 5° cooler near the tropopause than that of CWL while at higher altitudes the temperatures are the same. (3) The wavelength resolution of the solar flux is coarser in the CWL model with a different treatment of the Schumann-Runge bands. (4) The number of species integrated in the present model is about twice that of CWL (65 versus 32), and all species are integrated in both the time-dependent and steady state modes. (5) The diurnal averaging technique differs between the two models.

Items 2 and 4 do not appear to contribute significantly to the differences between the present calculation and that of CWL, whereas item 3 (the solar flux wavelength resolution) is a possible minor source of discrepancy. With the present model the effect of shifting the boundary altitude from 0 to 10 km is very difficult to assess quantitatively. The use of CWL's 10-km boundary altitude may alter the NO_x and HO_x interaction with ozone relative to the present model. The amount of odd nitrogen in the model can affect the degree of nonlinearity of the ozone response to increasing CIX [Prather et al., 1984]. The amount of N_2O in our model and that of CWL was 300 ppbv at the lower boundary, in agreement with the data in Figure 1-43 of the *World Meteorological Organization* [1981]. In our case, this leads to a maximum of about 20 ppbv of total odd nitrogen near 35 km. In order to examine the nonlinear response of ozone to large amounts of CIX, the CIX perturbation was extended to 30 ppbv ($\text{CIX} = 30 + 1.22 \text{ ppbv}$). The calculated results in the units of Figure 1 are 12.4% depletion in $\text{C}(\text{O}_3)$ at 11.3 ppbv $\Delta(\text{CIX})$, 19.4% at 15 ppbv, and 65.4% at 30 ppbv. The nonlinearity in the ozone depletion curve becomes significant in the range where the amount of CIX is comparable to or greater than the amount of NO_x [Prather et al., 1984].

From our investigation the calculated ozone perturbation was most sensitive to the choice of diurnal averaging method. Within the present model we compared the diurnal averaging technique used by CWL with the exact averages. This approximation [Turco and Whitten, 1978] is based on finding the ratios of the average daytime to average nighttime densities of each species in the model at each altitude. Although the lengths of the day and night are functions of altitude, a good fit to the exact results using a single parameter can be obtained by selecting 5 km as a reference altitude. Other choices of reference altitude for the length of the daytime lead to a wide range of calculated results. When the best fitting day-night ratio diurnal averages are used, the percentage change in the ozone column content above 10 km differs only a small amount from the exact calculation (e.g., -6.8% instead of -7.3% when CIX is 8.77 ppbv). However, there are larger differences in the density profiles, particularly above 35 km, and with some species at all altitudes (e.g., N_2O_3).

There are similar problems with approximating the diurnal averages of photolysis rates within the Schumann-Runge bands where the effective cross sections are a function of pressure and optical depth or at other wavelengths for processes with pressure-dependent cross sections. In these cases the convenient approximate formulation of Rundel [1977] breaks down with varying degrees of error.

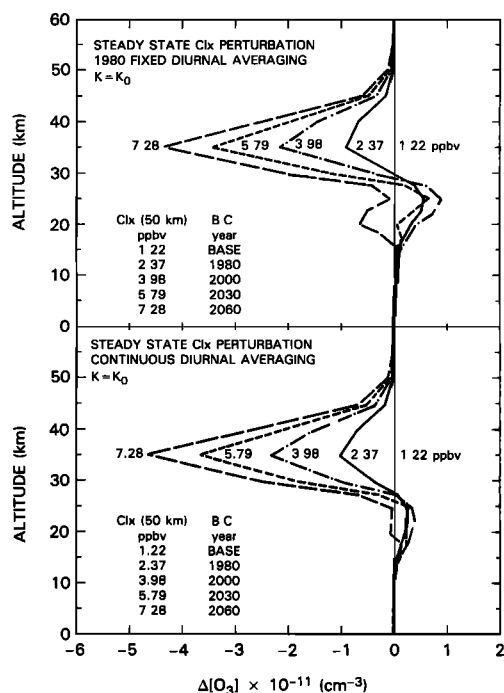


Fig. 5. The effect of different diurnal averaging methods on the calculated steady state change in ozone density as a function of altitude and ClX mixing ratio referenced to the case where the ClX mixing ratio at 55 km is 1.22 ppbv (no F-11 and F-12). The cases are labeled by their ClX mixing ratio at 55 km (2.37, 3.98, 5.79, and 7.28 ppbv) and result from boundary conditions appropriate for the years 1980, 2000, 2030, and 2060, respectively.

Since the ClX perturbation produces partially offsetting positive and negative ozone changes as a function of altitude as shown in Figure 5, a small difference in model behavior in the 15- to 25-km altitude range could account for the disagreement in the small ClX perturbation results. Figure 5 can be compared with Figure 3b of CWL. The magnitude and trend of the ozone changes above 35 km are approximately the same for the results from CWL and both types of diurnal averaging shown in Figure 5. When the diurnal averaging coefficients are held fixed for different amounts of ClX, the ozone response below 30 km is nonlinear. As small amounts of ClX are added to the reference atmosphere ($\mu(\text{ClX}) = 1.22$ ppbv), the ozone density below 30 km first increases and then begins to decrease for amounts of ClX in excess of 4 ppbv. It is this behavior that gives rise to the nonlinear response of ozone to ClX shown in Figure 1, case C. In contrast to this is the ozone response when the diurnal averaging is recomputed for each value of ClX. As shown in the bottom panel of Figure 5, the ozone density barely changes below 30 km for amounts of ClX up to about 6 ppbv. Since the response above 30 km is nearly a linear function of the ClX mixing ratio, the column content as shown in Figure 1 is also linear. As ClX increases above 6 ppbv, the small ozone density response below 30 km is dominated by the much larger response above 30 km. The net result is a linear decrease in column ozone with increasing ClX mixing ratios to the approximately 10 ppbv shown in Figure 1 and beyond.

The above discussion illustrates the sensitivity of the present calculation to various approximations to the diurnal averaging of photochemical reaction rates. None of the approximations that were tried yielded the nearly flat (and positive) response of total ozone column content for small amounts of ClX found by CWL.

Once the region of a small ClX perturbation is passed, the present model results for case C in Figure 1 using 1980 fixed diurnal averages are roughly parallel with those of CWL, but disagree in both form and magnitude with case A using continuously updated diurnal averages. For the assumed ClX growth rate, the present model and that of CWL (for $\mu(\text{ClX}) > 4.16$ ppbv) yield a percent change in the total column content of ozone with the ClX mixing ratio $\mu(\text{ppbv})$ that can be approximated by

Case A

$$\% \text{change}[C(\text{O}_3)] = -0.82107[\mu(\text{ClX}) - 1.22]^{1.069023} \quad (2a)$$

Case C

$$\% \text{change}[C(\text{O}_3)] = -0.179992[\mu(\text{ClX}) - 0.72]^{1.8269669} \quad (2b)$$

Case D (CWL model M)

$$\% \text{change}[C(\text{O}_3)] = -0.141833[\mu(\text{ClX}) - 3.368]^{2.15337} \quad (2c)$$

Insofar as the steady state results are concerned, the large ClX perturbation predictions of ozone trends from CWL and the present model agree only at their crossing point near 10 ppbv of ClX. For larger amounts of ClX the predictions of ozone depletion for the nonlinear results in case C and those of CWL rapidly exceed the nearly linear results of case A. If the concern is for early experimental detection of the ozone depletion due to chlorine injection, then the presence of a nearly zero-slope response curve in the region of positive change shown by CWL could be significant.

VERIFYING MODEL PREDICTIONS

To estimate when the decrease in ozone can be experimentally detected within the stratosphere, the ozone depletion rate was calculated with reference to a time-varying amount of ClX at 55 km arising from a specified rate of chlorine injection at the ground. The estimated dates in the following discussion refer only to the particular perturbations used in the model calculations. Other simultaneous perturbations to the atmosphere that are not considered here (e.g., increasing amounts of CO_2) may alter the specific prediction time scale.

The 55-km ClX growth curve is shown in Figure 6 for the present model study along with that of CWL originally obtained at 40 km from Logan *et al.* [1978]. The two growth curves should be comparable, since the ClX mixing ratio is nearly constant with altitude above 40 km. This model of halocarbon release (model B2 of Logan *et al.*, [1978], described in their Figure 27 and on page 223) assumes a continued release of F-11, F-12, and CCl_4 at 1974 rates with an increasing release rate of CH_3CCl_3 . Boundary conditions for F-11, F-12, and CH_3CCl_3 in terms of mixing ratios at 0 km are given by Logan *et al.* [1978] (see their Figure 39) and are approximately reproduced in Table 2. Since the concentration of CH_3CCl_3 is not explicitly computed in the present model, the chlorine content of CH_3CCl_3 was combined with that of CFCl_3 (F-11). The CCl_4 and CH_3Cl boundary conditions are held constant at 0.13 and 0.68 ppbv, respectively. The small increase in our ClX growth curve at 55 km needed to exactly match that of CWL would increase the disagreement in the ozone depletion rate between the two models at small values of ClX. For large values of ClX the growth curves gradually approach each other and cross. Within the range of the ClX

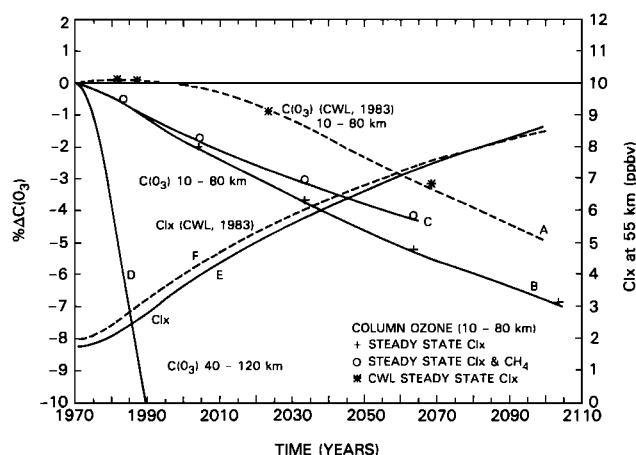


Fig. 6. The decrease in ozone column content between 10 and 80 km as a function of time based on a fluorocarbon release rate proposed by Logan *et al.* [1978] and a concurrent methane injection described by Keller *et al.* [1983]. The percentage change is referenced to the time-dependent ozone column content calculated for the year 1970. The figure shows $C(O_3)$ computed by CWL (shifted to refer to the year 1970) and the present model between 10 and 80 km, and $C(O_3)$ above 40 km. The graphs labeled A to F are (A) the time-dependent percentage change in ozone column content from Figure 4 of CWL, (B) the corresponding calculation from the present model, (C) the same as B, but with CH_4 added concurrently with the fluorocarbons, (D) the time-dependent percentage change in ozone column content above 40 km, (E) the CIX growth curve at 55 km, and (F) the CIX growth curve from Figure 4 of CWL. The points labeled by plus symbols are the percentage change in ozone column content from the steady state calculation for the same amount of CIX at 55 km as in the time-dependent model at the indicated point in time. The points labeled by circles are the same, but with CH_4 added.

mixing ratios considered here, the small differences between the CIX growth curves are unimportant. The chlorine injection rate indicated in Figure 6 leads to a long-term average 4.3% depletion from 1970 values in the total stratospheric ozone content by the year 2045, compared to approximately 1.5% as predicted by CWL. The percent changes in ozone given by CWL have been replotted in Figure 6 in relation to their 1970 value of $C(O_3)$. The main difference arises from the presence of a 35-year period of nearly flat and slightly positive change in O_3 column content for the initial phases of the CIX perturbation as calculated by CWL, compared to the immediate decrease found in the present calculation. At large values of CIX the ozone depletion curves shown in Figure 6 cross, so that ultimately CWL would predict a larger percent change in $C(O_3)$.

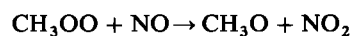
The ozone depletion curves for the years 1970 to 2100 were obtained by computing two diurnally averaged time-dependent cases. The first holds the solar declination and sun-earth distance fixed at the equinox value as time progresses, and the second allows the seasonal changes to occur. When every point is plotted, the seasonally calculated ozone depletion curves make relatively large oscillations about the fixed-sun equinox results with a peak-to-peak amplitude of about 30%. Alternately, from each case one data point can be selected per year at the date of the spring equinox for the purpose of plotting the results in the form of percent differences of $C(O_3)$ from its 1970 value. The resulting two curves are almost identical when plotted in this manner. In addition, each steady state calculation shown in Figure 1 can be associated with a particular year by matching the CIX mixing ratio at 55 km with the values from the CIX growth curve shown in Figure 6.

The resulting percent differences from 1970 (the plus symbols in Figure 6) are just slightly smaller than the percent differences from the seasonal calculation over the entire range of the CIX mixing ratio from 1.22 to 9 ppbv. The steady state ozone depletion values from Table 5 of CWL (shown as asterisks in Figure 6) are also nearly the same as their time-dependent values.

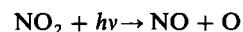
To achieve the same amount of CIX at 55 km, the mixing ratios of $CFCl_3$ and CF_2Cl_2 (F-11 and F-12) at the ground must be larger for the time-dependent case than for the steady state because of the relatively slow rate of vertical transport. Using the data in Table 2 to associate F-11 and F-12 mixing ratios with a particular year, the increase necessary to match CIX at 55 km is equivalent to about a 5-year delay relative to the steady state boundary condition values. The delay value grows to the nearly constant value of about 5 years by 1980 for calculations started using 1970 conditions.

The near identity of the two methods of obtaining spring equinox curves indicates that seasonal photochemical effects in the actual atmosphere are not likely to influence the long-term average rate of ozone depletion. Omitted from this calculation are the effects of atmospheric motions that shift the phase of the seasonal ozone maxima and minima relative to the seasonal variation of the solar flux. These other seasonal and apparently seasonal effects that are not annually cyclic (e.g., the so-called quasi-biennial oscillation) should cause variations from the idealized depletion curve in Figure 6 without affecting its long-term trend. Even though the system of equations describing the photochemical effects is nonlinear, cyclic perturbations of currently observed physical size (temperature, pressure, solar flux, winds, and boundary fluxes) produce cyclic chemical changes. An exception to the cyclic response is the small annual change in atmospheric minor constituent composition caused by changes in the removal rate of soluble gases in the troposphere by rain-out.

The total ozone perturbation due to the introduction of CIX can be significantly altered by the ground fluxes of other naturally or anthropogenically produced constituents. As a single example, the estimated increase in atmospheric methane at a rate of about 1.5% per year [Keller *et al.*, 1983] leads to an increase in ozone column content $C(O_3)$ that partially offsets the decrease by CIX. As shown in Figure 6 and Figure 1, the combined methane (22.5 ppbv per year) and CIX perturbation may cause a smaller decrease of 3.5% in $C(O_3)$ by the year 2045, compared to the 4.3% decrease due to CIX alone. The percent changes are calculated in relation to the same reference atmosphere with 1.22 ppbv CIX at 55 km and 1.5 ppmv CH_4 at the ground. Up to an altitude of about 40 km the addition of methane produces a slightly smaller but qualitatively similar percent change in the ozone column content. The small difference is due to the removal of Cl by the reaction $CH_4 + Cl \rightarrow HCl + CH_3$. There is also a small increase in tropospheric ozone arising from photooxidation of the increasing amount of CH_4 . The methane photooxidation results in CH_3OO and then in the production of additional NO_2 :



followed by



producing a net increase in ozone.

Above about 45 km the difference in the CIX perturbation

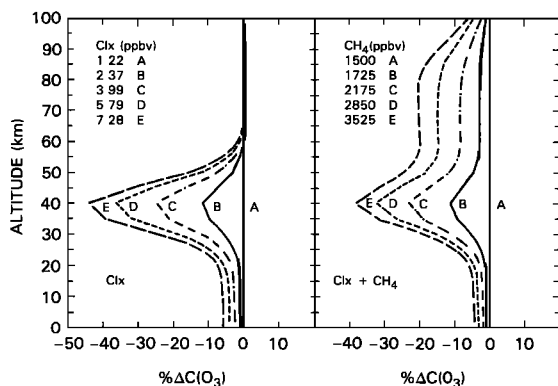


Fig. 7. The percentage change in column ozone with varying amounts of CIX at 55 km calculated in the steady state mode, with and without additional CH_4 . The association of the amounts of CIX and CH_4 is taken from the time-dependent calculation shown in Figure 6 and the reported 1.5% per year rate of increase for CH_4 [Keller *et al.*, 1983]. The change in total ozone column content by the introduction of CH_4 is mostly determined in the region below 45 km where increasing methane causes an increase in ozone.

with increasing methane becomes significant because of the additional HO_x produced (see Figure 7). At 55 km, increasing the amount of CIX to about 4.0 ppbv (about the year 2005) alone produces only a 3% negative change in $\text{C}(\text{O}_3)$, compared to a 9% negative change for the same CIX perturbation when CH_4 is increased from 1.5 to 2.18 ppmv at the ground (curves C of Figure 7). The effect on ozone of a combined methane and CIX perturbation dominates that due to CIX alone down to about 45 km, so that satellite observations of an ozone reduction at these altitudes cannot be simply associated with CIX even in the absence of other known perturbing effects. Since the chlorine effect on $\text{C}(\text{O}_3)$ discussed here dominates that due to the increasing amount of methane below 45 km, the basic problem of detecting the ozone change due to CIX remains, with some added complications in interpreting the data.

The experimental detection of these effects is most likely to be obtained from satellite observations (e.g., Nimbus 7). These observations are more sensitive to changes in the 35- to 40-km altitude range rather than near the ozone density maximum. Accordingly, we have computed the expected depletion of the ozone column above 40 km (see Figure 6) and have obtained results that approximately agree with most other model calculations. As expected from the shorter chemical time constants for ozone destruction at higher altitudes, the predicted change reaches about 6.8% by the year 1985 relative to 1970 as a reference point, or in about 12 years relative to the 1980 column content. In spite of some difficulties from competing effects similar to that discussed for methane (e.g., increasing CO_2 , NO_x , and average temperature changes), the altitude range from 35 to 45 km should provide the earliest indication of CIX-induced ozone destruction.

Although early detection of ozone changes associated with CIX is of theoretical interest, the real concern is with the possible reduction in total ozone column content. Detection of small total ozone changes within a latitude band requires that seasonal and other short-period variations be carefully removed from the data. For example, the Nimbus 4 total ozone data show a daily fluctuation of about 8% and a seasonal variation of nearly 30% at 35°N latitude. Even after removal of these short-term variations, if the expected secular (e.g.,

11-year cycle) solar ultraviolet flux variability or long-term temperature variations are sufficiently large, the ozone reduction due to chlorine could be masked during the ascending phase of the ozone response to a particular cycle and accentuated on the descending phase. At the present time there are insufficient satellite data to establish the existence of a long-term cycle that affects ozone. In addition, any such effect is likely to be small, since the ground-based data presented by the *World Meteorological Organization* [1981, chapter 3] indicate that the amplitude of any long-term variations would have to be 2% or less for the variability not to be present in the existing record. This conclusion is supported by an analysis of the ground-based Umkehr ozone data by Reinsel *et al.* [1983, 1984]. They found that the total column content of ozone showed no significant variation while the 38- to 43-km data showed a -3.33% change (from -1.03 to -5.63%) over the time period 1970 to 1980. They concluded that the larger downward trend in the Nimbus 4 backscattered ultraviolet (BUV) ozone data is probably due in large part to drift in the BUV instrument. The results from the present model calculation for the same time period yield a change in the column content above 40 km of about -6% for CIX alone, and -5.5% for the combined CIX and CH_4 perturbation.

In the vicinity of 40 km the ozone density and temperature are each positively proportional to the solar flux variations, with ozone negatively proportional to the temperature changes, so that one effect may partially cancel the other. An examination of the Nimbus 4 ozone mixing ratio at 2 mbar pressure and lower (~40 km and above) indicates that ozone seems to follow the sunspot and 10.7-cm flux indices [Chandra, 1984]. The possible correlation is suggestive of long-term solar flux variability. However, Chandra demonstrates that the ozone does not necessarily track the short-term variations in the sunspot number and 10.7-cm flux indices. Similar partial correlations are present in the more recent Nimbus 7 data record.

At present the secular change in UV solar flux between 180 and 320 nm is not established by the existing solar flux data record. We know neither the magnitude nor whether the phase of the solar flux change is the same as that of the solar sunspot index usually used to follow the 11-year cycle. For wavelengths longer than 320 nm there appears to be no suggestion of any variation associated with the 11-year cycle. Preliminary analysis of the Nimbus 7 UV data by D. F. Heath (personal communication, 1983) indicates that the 11-year cycle may have a flux variation for wavelengths between 180 and 320 nm at least as large as the observed 27-day cycle [Heath and Schlesinger, 1983]. If this is the case, then the model calculations indicate that the long-wavelength spectral shape must fall off more sharply than suggested by Heath and Schlesinger to match the observed lack of 27-day variation in the total column ozone greater than the 2% lower limit of observational sensitivity in the ground-based data.

In order to model the effect of a small long-period cyclic change on the observability of the CIX-induced reduction of ozone, we assume that the spectral shape of Heath and Schlesinger's [1983] 27-day cycle can be applied to the 11-year cycle and that it is in phase with the sunspot index. A hypothetical representation of a small modulation of the solar flux might be given by

$$F(t, \lambda) = F_0(\lambda) \{1 + B(\lambda) \sin [2\pi(t - 1978.5)/11]\} \quad (3)$$

where $F_0(\lambda)$ is the reference solar flux above the atmosphere, t

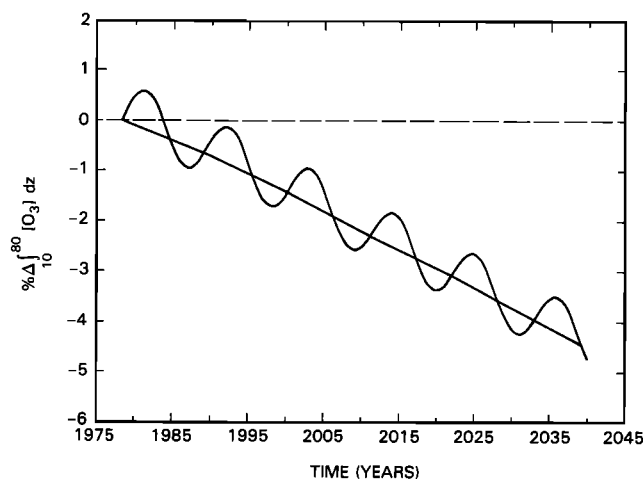


Fig. 8. The time-dependent percentage change in $C(O_3)$ between 10 and 80 km arising from the increasing amount of ClX, with a superimposed hypothetical 11-year solar cycle variation in the solar ultraviolet flux.

is time in years, and

$$\begin{aligned} B(\lambda) &= 0.002 & 290 < \lambda < 320 \text{ nm} \\ B(\lambda) &= 0.006 & 255 < \lambda < 290 \\ B(\lambda) &= 0.012 & 207 < \lambda < 255 \\ B(\lambda) &= 0.028 & 165 < \lambda < 207 \end{aligned}$$

The change in the ozone column content arising from the ClX perturbation and the varying solar flux is shown in Figure 8. The selection of an amplitude factor of about 40% of the 27-day cycle yields an ozone column content variation of about 1.5%. This is just below the 2% level of detectability in the existing total ozone data. However, the change is just large enough to compete with the predicted short-term ClX ozone destruction effect. With this or a similar long-term cyclic perturbation, at least 1.5 cycles of data would have to be obtained before the cyclic perturbations of ozone could be removed from that caused by ClX. In the present example this means a delay of about 17 years before an observed ozone change could be reliably associated with ClX, even in the absence of other interfering effects.

A 5% long-term (two or more solar cycles) change in ozone column content should be easily detectable with present satellite instrumentation. However, certain other physical processes can mask the unambiguous association of an observed depletion with chlorine injection at the 5% level. A temperature change of a few degrees Kelvin will produce a significant ozone perturbation that may have the same or opposite sign relative to the temperature change depending on altitude. The left panel of Figure 9 shows the effect of a uniform $+4^\circ$ temperature perturbation applied between the altitudes 20 and 120 km from both a steady state model calculation and a simple temperature-dependent chemical equilibrium equation for ozone density (equation (4)). A similar 1° temperature perturbation produces about a 1% decrease in the column ozone above 10 km. The result shows that the ozone percentage decrease is nearly a linear function of the small temperature increase. The size of this ozone perturbation is large enough to compete with the changes caused by the increasing amount of ClX. A corresponding small temperature decrease ($T - 4^\circ$) would produce almost the same changes as shown in the left

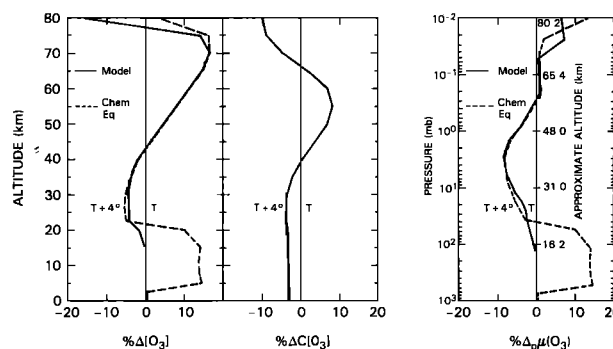


Fig. 9. The percent change in the ozone density and column content for a uniform 4° increase in temperature between 20 and 120 km. The steady state model results are compared with a simple chemical equilibrium calculation for an O_x , HO_x , NO_x , and ClX atmosphere. The same data are replotted as percent change in ozone mixing ratio on constant pressure surfaces showing the more familiar negative correlation with temperature changes seen in satellite data. The apparent difference in the temperature response arises from the change in the total density M when comparing ozone mixing ratios on constant pressure surfaces.

panel of Figure 9, but with opposite sign. Most short-term observed temperature changes are of mixed character, with the change in the upper stratosphere having the opposite sign compared to the lower stratosphere. The total ozone column content is affected more by temperature changes in the lower stratosphere than by those at higher altitudes. Except in unusual circumstances the effect of observed altitude-dependent temperature changes on the total ozone column content should not be offsetting.

The specific ozone changes seen at different altitudes above 25 km are governed by simple photochemistry for the ClX, methane, temperature, and other similar perturbations. For example, the largest temperature effect in the lower stratosphere arises from the temperature dependence of the Chapman mechanism reactions ($O + O_2 + M \rightarrow O_3 + M$ and $O + O_3 \rightarrow O_2 + O_2$ with rates k_2 and k_3 , respectively). In the upper stratosphere and lower mesosphere the Chapman chemistry temperature dependence is strongly modified by the HO_x chemistry. This is shown by examining the temperature dependence of the chemical equilibrium expression, equation (4), for ozone density for the reaction set given in Table 3. Reactions

TABLE 3. Reaction Rates

Reaction	Rates
$O + O_2 + M \rightarrow O_3 + M$	$k_2 = 6.0 \times 10^{-34}(300/T)^{2.3}$
$O + O_3 \rightarrow O_2 + O_2$	$k_3 = 1.5 \times 10^{-11}e^{-2218/T}$
$O_2 + h\nu \rightarrow O + O$	J_2
$\rightarrow O(^1D) + O$	
$O_3 + h\nu \rightarrow O(^1D) + O_2(^1\Delta)$	J_3
$\rightarrow O + O_2$	
$H + O_2 + M \rightarrow HO_2 + M$	$a_1 = 5.5 \times 10^{-32}(300/T)^{1.4}$
$H + O_3 \rightarrow OH + O_2$	$a_2 = 1.4 \times 10^{-10}e^{-470/T}$
$OH + O \rightarrow H + O_2$	$a_3 = 2.2 \times 10^{-11}e^{-117/T}$
$OH + O_3 \rightarrow HO_2 + O_2$	$a_4 = 1.6 \times 10^{-12}e^{-940/T}$
$HO_2 + O \rightarrow O_2 + OH$	$a_5 = 3.0 \times 10^{-11}e^{200/T}$
$HO_2 + O_3 \rightarrow HO + 2O_2$	$a_6 = 1.4 \times 10^{-14}e^{-580/T}$
$NO_2 + O \rightarrow NO + O_2$	$b_3 = 9.3 \times 10^{-12}$
$NO + O_3 \rightarrow NO_2 + O_2$	$b_4 = 2.2 \times 10^{-12}e^{-1430/T}$
$NO_2 + h\nu \rightarrow NO + O$	J_n
$Cl + O_3 \rightarrow ClO + O_2$	$d_2 = 2.8 \times 10^{-11}e^{-257/T}$
$ClO + O \rightarrow Cl + O_2$	$d_3 = 7.7 \times 10^{-11}e^{-130/T}$
$ClO + NO \rightarrow Cl + NO_2$	$d_4 = 6.2 \times 10^{-12}e^{294/T}$

All reaction rates are in cgs units, cm^3/s , cm^6/s , or s^{-1} .

appearing in Table 3 that do not explicitly appear in (4) were used in the derivation, but canceled algebraically. The importance of the individual terms can be assessed using the form $T/[O_3]d[O_3]/dT$.

$$\begin{aligned} [O_3]^2 &= \frac{C}{1 + g/[O_3]} \\ [O_3] &= 0.5[-g + (g^2 + 4C)^{1/2}] \end{aligned} \quad (4)$$

where

$$\begin{aligned} C &= \frac{J_2[O_2]^2 M k_2}{J_3 k_3 (1 + h)} \\ h &= \frac{a_6[OH] + b_4[NO] + d_2[Cl]}{J_3} \\ g &= g_1 + g_2 \\ g_1 &= \frac{n}{k_3} \left[1 + \frac{a}{J_3(1 + h)} \right] \\ n &= b_3[NO_2] + a_7[HO_2] + d_3[ClO] \\ a &= a_2[H] + a_8[HO_2] \\ g_2 &= \frac{J_2[O_2]k_3 + k_2[O_2]Ma}{k_3 J_3 (1 + h)} \end{aligned}$$

For a typical case, h is less than 0.011 ($h = 0.01$ at $z = 35$ km), and a is less than 0.181 ($a = 0.18$ at $z = 80$ km). The quantity g_2 is important below about 65 km; otherwise, $g = n/k_3$. Various approximations can be made when deriving (4) from the assumed set of reactions that give rise to useful and simpler forms. One example of a simplified form of (4) is given by Nicolet [1975, equation 99]. In the case of Nicolet's form and a similar one suggested by H. S. Johnston (personal communication, 1984), the numerical results closely approximate the exact result given in (4) above about 25 km. Below 30 km, transport effects (represented by a diffusion term in a one-dimensional model) are increasingly important, so that all three chemical equilibrium forms start to fail when density values from the complete numerical model are used to calculate $[O_3]$.

Since transport effects are omitted from (4), the ozone altitude profile calculated from (4) begins to differ below 30 km from the ozone profile calculated using the numerical model. The temperature dependence of the percent difference (using (4)) shown in the left panel of Figure 9 is nearly identical in the stratosphere and lower mesosphere because the same chemistry is dominant in both the model and the simple equilibrium expression. Above 25 km the assumed invariant diffusion model has almost no effect on the percentage change due to temperature and other photochemical perturbations. It should be pointed out that the positive correlation of the ozone density with temperature changes in the upper stratosphere and mesosphere shown in the left panel of Figure 9 does not appear to be the result usually seen in satellite data. Most often the data are presented as ozone mixing ratios plotted on a constant pressure scale. Accordingly, the right panel of Figure 9 shows the same data replotted to show the more conventional negative correlation of the ozone mixing ratio at most pressure altitudes. The apparently different results for the same data arise from the different values of the total density M associated with a constant pressure surface when the temperature changes.

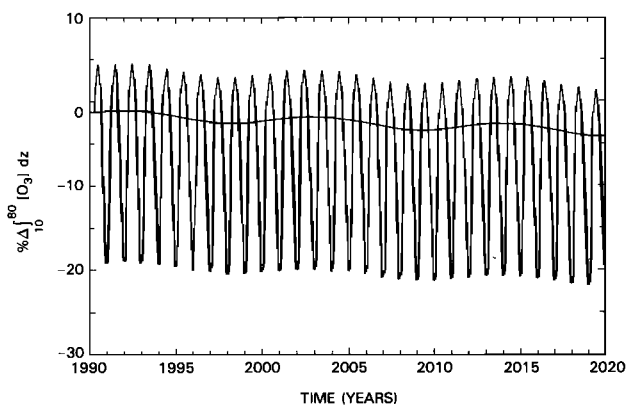


Fig. 10. The effect of the combined solar cycle variation and the seasonal variation. The 30% peak-to-peak variation between summer and winter compares favorably with the observed variation in the Nimbus 4 total ozone data. The slowly varying curve connects the spring equinox points.

If there is a long-term secular change in the solar flux similar to the above hypothetical 11-year UV flux solar cycle, the resulting positively correlated ozone change would easily mask the chlorine perturbation until well after 1985. Figure 10 shows a simple example of the masking effect of combining the small hypothetical solar cycle effect, the seasonal effect, and the ClX perturbation. The effects of changing temperature are not included. Also shown is the trend curve formed by connecting the spring equinox points. The amplitudes of the calculated percentage ozone changes are very similar to the mid-latitude ($35^\circ N$) Nimbus 4 data over a comparable time period. The exact phase relationship with respect to the solar declination angle (or annual day number) is not reproduced from a one-dimensional model. If a small random or systematic error is introduced into the exact periodicity of the simulated data, the trend curve may be distorted enough to completely mask the predicted ozone changes for many years. This problem may be partially avoided by forming running near-annual averages of the data indexed to the summer ozone maxima.

Removal of the daily and seasonal variations from the Nimbus 4 ozone column content data [Chandra, 1984] shows that the ozone column content follows the trend in the solar sunspot index and 10.7-cm flux, but not their short-term variations. These periodic and aperiodic ozone variations are likely due to atmospheric dynamical effects (winds and temperature). The Nimbus 4 data record does not cover a sufficient period of time to allow the removal of these additional variations and still be able to show the smaller ClX perturbation. The predicted change in the total ozone column content is too small at present to be seen in the data obtained over a very long period of time from ground-based measurements.

Because of the several masking or competing effects, detection of a long-term trend does not in itself verify the influence of ClX on atmospheric ozone. However, we suggest that with increasing amounts of ClX entering the atmosphere it should be possible to detect a signature of the ClX destruction of ozone in its diurnal cycle at approximately double the present amount of ClX. Pallister and Tuck [1983] have shown that the introduction of very large amounts of ClX into the atmosphere severely distorts the percentage change diurnal variation of ozone (relative to midnight values). Their calculations of the low ClX case agree with the earlier calculations of Herman [1979a]. Since the laboratory chemistry rates for the

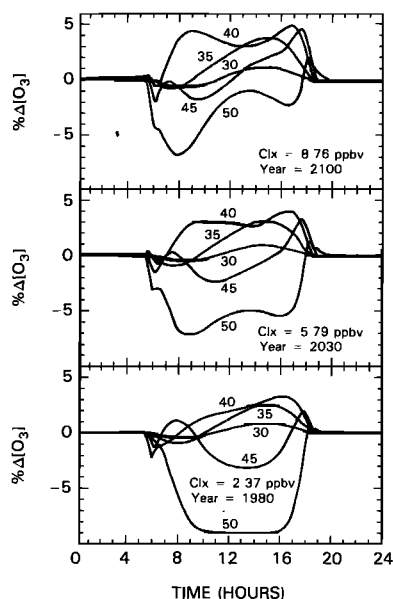


Fig. 11. The percent change in diurnally varying ozone density for the altitudes 30, 35, 40, 45, and 50 km referenced to the midnight value for each altitude. The three sets show the effect of the increasing amount of CIX on the shape of the percent change curves. The 40-km curve shows a significant change in the morning to afternoon ratio when CIX reaches about 5 ppbv.

stratosphere have changed considerably in the time period between the two publications, the agreement demonstrates the lack of sensitivity of the midday percentage change results to the precise chemistry rates assumed in a given model. We have investigated this sensitivity to perturbations in the reaction rates of the order of the published error limits and have found that the resulting changes in the diurnal variation of ozone are much smaller than the changes due to the CIX perturbation. The same insensitivity is present for small perturbations in temperature (we investigated a 4°K change) and the assumed solar flux. The introduction of increased amounts of CO₂ and N₂O causes changes in the ozone density, but little change in the diurnal variation. If the amount of gas phase water in the upper stratosphere changes significantly (e.g., in response to increased CH₄) the shape of the diurnal ozone cycle is altered, but the CIX signature is still present. Figure 11 shows the changes in the ozone diurnal variation due to the increasing CIX for three cases based on the growth rates given by Logan *et al.* [1978]. These are (1) CIX corresponding to current levels (~2.4 ppbv), (2) CIX corresponding to the predicted amount in the year 2030 (~5.8 ppbv), and (3) CIX corresponding to the year 2100 (~8.8 ppbv). Case 1 shows agreement with the earlier results of Herman [1979a] and Pallister and Tuck [1983].

Case 3, with a large CIX perturbation, and case 2, at half the change in CIX from 1970 values, both show a strong signature relative to case 1. By combining ozone depletion data from 40 km with measurements of the morning to afternoon ratios of ozone from a limb-viewing satellite experiment, the influence of CIX on ozone may be detected well before the year 2030. This would still be before the reduction of the total ozone column content, due to increasing amounts of CIX, can be detected. Although the changes in total column ozone are only weakly affected by ozone destruction above 40 km, confirmation of the predictions of the early effects of halocarbon injection is important for the assessment of the long-term predictions.

CONCLUSION

The response of stratospheric ozone to the injection of chlorine-bearing compounds has been investigated using a one-dimensional time-dependent photochemical model. The present investigation does not verify the presence of a nonlinear response function of the ozone column content with changes in the amount of CIX between 1.2 and 10 ppbv in the upper stratosphere as described by CWL. We also did not find a broad region of increase in ozone column content for small amounts of CIX, or a region of nearly zero slope. Instead we find an immediate nearly linear decrease in the ozone column content as a function of the change in the CIX mixing ratio when the diurnal averages are continuously updated. For larger CIX perturbations, when the amount of CIX is comparable to the amount of NO_x near 35 km, the change in C(O₃) is a nonlinear function of the change in CIX, in agreement with the results of Prather *et al.* [1984]. The main consequences are the prediction of a detectable decrease in stratospheric ozone at an earlier date than that of CWL, and a smaller C(O₃) decrease for large values of CIX. Satellite detection of this decrease should occur first in the 40-km region by 1987–1990, although it may be obscured until a later date by seasonal and longer-term atmospheric variations. If the growth of CIX in the atmosphere is similar to that suggested by Logan *et al.* [1978], the reduction of the total ozone column content in the stratosphere by about 5% will probably not occur until much later (about the year 2050).

Even after removal of the short- and long-term variations from the ozone data, an observed decrease in ozone column content of from 5 to 10% over the next several decades may be due to causes other than CIX introduced into the atmosphere [Logan *et al.*, 1978]. An example is the increase in [CH₄] at a rate of 1.5% per year [Keller *et al.*, 1983], leading to a partially offsetting increase in C(O₃) relative to the CIX-induced decrease. The diurnal variation of ozone may afford a method to associate changes in ozone content with the presence of large amounts of CIX in the stratosphere. At approximately 5 ppbv CIX the ratio of morning to afternoon ozone density at about 40 km changes sufficiently from current values to be detected with satellite instruments (e.g., Nimbus 7). On the basis of the present calculations, the change in this ratio is not sensitive to moderate changes in the chemical reaction rates, small changes in atmospheric temperature, or small changes in solar flux.

REFERENCES

- Ackerman, M., Ultraviolet solar radiation related to mesospheric processes, in *Mesospheric Models and Related Experiments*, edited by G. Fiocco, Springer, New York, 1971.
- Allen, M., and J. E. Frederick, Effective photodissociation cross sections for molecular oxygen and nitric oxide in the Schumann-Runge bands, *J. Atmos. Sci.*, **39**, 2066–2075, 1982.
- Carnahan, B., H. A. Luther, and J. O. Wilkes, *Applied Numerical Methods*, John Wiley, New York, 1969.
- Chandra, S., An assessment of possible ozone-solar cycle relationship inferred from Nimbus 4 BUV data, *J. Geophys. Res.*, **89**, 1373–1379, 1984.
- Cicerone, R. J., S. Walters, and S. C. Liu, Nonlinear response of stratospheric ozone column to chlorine injections, *J. Geophys. Res.*, **88**, 3647–3661, 1983.
- Heath, D. F., and B. M. Schlesinger, Global response of stratospheric ozone to ultra-violet solar flux variations on active region time scales (abstract), *Eos Trans. AGU*, **64**, 780, 1983.
- Herman, J. R., The response of stratospheric constituents to a solar eclipse, sunrise, and sunset, *J. Geophys. Res.*, **84**, 3701–3710, 1979a.
- Herman, J. R., The problem of nighttime stratospheric NO₃, *J. Geophys. Res.*, **84**, 6336–6338, 1979b.
- Herman, J. R., and J. E. Mentall, O₂ absorption cross sections (187–

- 225 nm) from stratospheric solar flux measurements, *J. Geophys. Res.*, **87**, 8967–8975, 1982.
- Keller, M., T. J. Goreau, S. C. Wofsy, W. A. Kaplan, and M. B. McElroy, Production of nitrous oxide and consumption of methane by forest soils, *Geophys. Res. Lett.*, **10**, 1156–1159, 1983.
- Kley, D., E. J. Stone, W. R. Henderson, J. W. Drummond, W. J. Harrop, A. L. Schmeltekopf, T. L. Thompson, and R. H. Winkler, In situ measurements of the mixing ratio of water vapor in the stratosphere, *J. Atmos. Sci.*, **36**, 2513–2524, 1979.
- Logan, J. A., M. J. Prather, S. C. Wofsy, and M. B. McElroy, Atmospheric chemistry: Response to human influence, *Philos. Trans. R. Soc. London*, **290**, 187–234, 1978.
- Molina, M. J., and F. S. Rowland, Stratospheric sink for chlorofluoromethanes: Chlorine atom catalysed destruction of ozone, *Nature*, **249**, 810–812, 1974.
- NASA/Jet Propulsion Laboratory (JPL), Chemical kinetics and photochemical data for use in stratospheric modelling, evaluation no. 5, NASA panel for data evaluation, *JPL Publ. 82-57*, Pasadena, Calif., 1982.
- NASA/Jet Propulsion Laboratory (JPL), Chemical kinetics and photochemical data for use in stratospheric modelling, evaluation no. 6, NASA panel for data evaluation, *JPL Publ. 83-62*, Pasadena, Calif., 1983.
- Nicolet, M., Stratospheric ozone: An introduction to its study, *Rev. Geophys. Space Phys.*, **13**, 593–636, 1975.
- Pallister, R. C., and A. F. Tuck, The diurnal variation of ozone in the upper stratosphere as a test of photochemical theory, *Q. J. R. Meteorol. Soc.*, **109**, 271–284, 1983.
- Plass, G. N., G. W. Kattawar, and F. E. Catchings, Matrix operator theory of radiative transfer, 1, Rayleigh scattering, *Appl. Opt.*, **12**, 314–329, 1973.
- Prather, M. J., M. B. McElroy, and S. C. Wofsy, Reduction in ozone at high concentrations of stratospheric halogens, *Nature*, **312**, 227–231, 1984.
- Reinsel, G., G. C. Tiao, R. Lewis, and M. Bobkoski, Analysis of the upper stratospheric ozone profile data from the ground-based Umkehr method and the Nimbus 4 BUV satellite experiment, *J. Geophys. Res.*, **88**, 5393–5402, 1983.
- Reinsel, G., G. C. Tiao, J. J. DeLuise, C. L. Mateer, A. J. Miller, and J. E. Frederick, Analysis of upper stratospheric Umkehr ozone profile data for trends and the effects of stratospheric aerosols, *J. Geophys. Res.*, **89**, 4833–4840, 1984.
- Rundel, R. D., Determination of diurnal average photodissociation rates, *J. Atmos. Sci.*, **34**, 639–641, 1977.
- Turco, R. P., and R. C. Whitten, A note on the diurnal averaging of aeronautical models, *J. Atmos. Terr. Phys.*, **40**, 13–20, 1978.
- World Meteorological Organization, The stratosphere 1981, theory and measurements, *Rep. 11*, Geneva, 1981.
- Wuebbles, D. J., Chlorocarbon emission scenarios: Potential impact on stratospheric ozone, *J. Geophys. Res.*, **88**, 1433–1443, 1983.

J. R. Herman and C. J. McQuillan, NASA Goddard Space Flight Center, Code 616, Greenbelt, MD 20771.

(Received February 13, 1984;
revised November 29, 1984;
accepted January 4, 1985.)